Magnetism of uranium/iron multilayers: II. Magnetic properties

2004 J. Phys.: Condens. Matter 16 8507

(http://iopscience.iop.org/0953-8984/16/47/005)

INSTITUTE OF PHYSICS PUBLISHING JOURNAL OF PHYSICS: CONDENSED MATTER

J. Phys.: Condens. Matter **16** (2004) 8507–8518 PII: S0953-8984(04)84355-8

Magnetism of uranium/iron multilayers: II. Magnetic properties

A M Beesley[1,7], S W Zochowski[2], M F Thomas[1], A D F Herring[1], S Langridge[3], S D Brown[1,4], R C C Ward[5], M R Wells[5], R Springell[2], W G Stirling[1,4] and G H Lander[6]

[1] Department of Physics, University of Liverpool, Liverpool L69 7ZE, UK
[2] Department of Physics and Astronomy, University College London, London WC1E 6BT, UK
[3] ISIS, Rutherford Appleton Laboratory, Chilton, Oxfordshire OX11 0QX, UK
[4] European Synchrotron Radiation Facility, BP220, F-38043 Grenoble Cedex 09, France
[5] Clarendon Laboratory, University of Oxford, Oxford OX1 3PU, UK
[6] European Commission, JRC, Institute for Transuranium Elements, Postfach 2340, Karlsruhe, D-76125, Germany

E-mail: amb@cmp.liv.ac.uk

Received 3 August 2004, in final form 4 August 2004
Published 12 November 2004
Online at stacks.iop.org/JPhysCM/16/8507
doi:10.1088/0953-8984/16/47/005

Abstract

Well-defined U/Fe multilayers of varying layer thicknesses and bilayer repeat numbers were prepared by a dc magnetron sputtering method. Polarized neutron reflectometry, off-specular neutron diffraction and magnetic moment measurements were used to determine the physical properties of the multilayers leading to an evaluation of the magnetic moments associated with the U and Fe atoms. The multilayers exhibit ferromagnetic behaviour with the easy axis in the plane of the multilayer. The saturation magnetization was found to increase with increasing Fe-layer thickness and the magnetic moment averaged over the structured iron layers was below the bulk value of 2.2 μ_B/Fe atom. No anomalies were observed in the magnetization from 4.2 to 375 K in temperature-dependent scans at 0.005 and 0.1 T or in magnetic field scans from 0 to 7 T at 4.2 and 295 K. The hysteresis curves exhibited a small degree of perpendicular magnetic anisotropy. The Curie temperatures for the multilayers were determined from ac susceptibility measurements and were found to be less than the bulk Fe value of 1043 K.

(Some figures in this article are in colour only in the electronic version)

[7] Author to whom any correspondence should be addressed.

1. Introduction

Magnetic multilayers have recently attracted a great deal of interest, based not only on their potential technical applications, but also on understanding the fundamental mechanisms of their magnetic properties. Multilayers with the easy axis of magnetization perpendicular to the multilayer plane, as in Pd/Co [1], are useful for magneto-optical storage devices. Magnetic films with a high saturation magnetization and good soft-magnetic properties (low coercivity and high permeability) are most suitable for high linear density recording. The phenomenon of giant magnetoresistance, initially found in Cr/Fe [2], has also given rise to much research into multilayer magnetism.

Interest in rare-earth multilayers arises because of earlier interest in Ce-based multilayers [3] where there is a strong interaction between the delocalized 4f electrons of Ce and the 3d electrons of transition metals, giving rise to interesting properties. A natural extension of this body of work is to place 5f elements in multilayer structures. The magnetism of uranium compounds ranges in nature from localized, as in UO_2, to itinerant, as in UFe_2, to heavy fermion, as in UPt_3. Although uranium itself is non-magnetic, magnetism in uranium compounds is defined by the large orbital moment of the 5f electrons, with attendant large anisotropies, and strong hybridization that occurs between the 5f electrons and the valence band states of neighbouring atoms. Accordingly, the study of uranium-based multilayers is a potentially important extension of multilayer studies. Even though a study of UAs/Co multilayers showed that the uranium atom could carry a magnetic moment [4], there has been little work done on the behaviour of uranium-based multilayers.

We have already observed, by means of resonant x-ray scattering (RXS) tuned to the M_4 edge of uranium, a polarization of the 5f electrons at the U atoms, at room temperature and below, but the magnitude cannot be determined simply by the RXS technique [5]. In the present paper, we report results on the magnetic properties of U/Fe multilayers as determined by polarized neutron reflectometry (PNR), magnetization, and ac susceptibility measurements. In the preceding paper [6], hereafter referred to as paper I, we have described the preparation and structural characterization of these multilayers in some detail.

2. Experiment

The U/Fe multilayer samples used in this study were made in a two-gun dc sputtering system, which could be baked to give a vacuum of 2×10^{-10} mbar. The sputtering system had an ambient temperature rotating mount for two substrates. Deposition from high purity targets (>99.9%) was made at calibrated rates of approximately 3.5 Å s^{-1} onto glass substrates in an Ar pressure of 5×10^{-3} mbar. The fitted thicknesses ranged from 14 to 66 Å (±2 Å) for the U layers and from 9 to 108 Å (±2 Å) for the Fe layers, with the number of bilayer repeats ranging from 10 to 100. Table 1 lists the established layer thicknesses for the set of samples used in this study. X-ray and neutron reflectivity, x-ray diffraction and Mössbauer spectroscopy were used to determine the layer thicknesses, interface thickness and compositions of the U/Fe multilayers as discussed in paper I [6].

Polarized neutron reflectivity measurements on selected multilayers were performed on the D17 instrument at the reactor of the Institut Laue-Langevin, Grenoble, France, with a fixed wavelength of 5.3 Å (4% base resolution), and on the time-of-flight CRISP reflectometer at the ISIS pulsed neutron source at the Rutherford Appleton Laboratory, UK. All scans were taken at room temperature in a saturation field of 0.05 T.

A Quantum Design MPMS-7 SQUID magnetometer and an Aerosonic VSM 3001 were used to make the dc magnetization measurements. With the SQUID, magnetization

Table 1. Magnetic data from PNR, Mössbauer and SQUID magnetometry measurements. Fe- and U-layer thicknesses, t_{Fe} and t_U, respectively, bilayer repeats n, average number density N, percentage magnetic component from Mössbauer spectra, Fe magnetic moment data from the fits to the PNR scans of figure 1, using the three-layer model, and the magnetic moments per Fe atom from SQUID measurements. Note that this Fe moment is an average over the central and outer parts of the Fe layer; see the inset of figure 2. In each case the U moment is less than the estimated uncertainty of 0.05 μ_B in the PNR fits.

Sample	$t_{Fe} \pm 2$ (Å)	$t_U \pm 2$ (Å)	Bilayer repeats	$N \times (10^{28})$ Fe (at m^{-3})	Mössbauer magnetic interface (%)	PNR magnetic moment/Fe atom (μ_B)	SQUID magnetic moment/Fe atom (μ_B)
2.4	108	41	21	7.88	87	1.77 ± 0.05	1.79 ± 0.05
2.8	76	38	21	7.90	86	1.78 ± 0.05	1.72 ± 0.05
2.3	70	66	20	7.60	85	1.70 ± 0.06	1.64 ± 0.06
2.1	47	23	10	7.60	75	1.55 ± 0.09	1.60 ± 0.09
2.5	46	65	20	7.30	73	1.40 ± 0.05	1.48 ± 0.05
2.10	40	18	31	6.67	72	1.21 ± 0.05	1.12 ± 0.05
2.11	35	14	30	7.37	70	1.14 ± 0.05	1.25 ± 0.06
2.12	30	21	31	6.50	64	1.03 ± 0.06	0.95 ± 0.06
3.2	19	28	60	6.00	10	0.23 ± 0.17	0.16 ± 0.06
3.4	9	40	100	6.00	10	0.24 ± 0.17	0.24 ± 0.17

measurements were taken at temperatures from 4.2 to 375 K, at 0.5 K s^{-1}, and in magnetic fields, changing at a rate of 0.003 T s^{-1} from 0 to 7 T, applied parallel to the surface of the multilayers. The VSM was used at room temperature at fields below 0.5 T, with $\Delta H/\Delta t$ approximately equal to 0.002 T s^{-1}. Measurements with the VSM could be made with the applied magnetic field both parallel and perpendicular to the plane of the multilayer. A Geofyzika Kappabridge KLY-2.1 susceptometer was used to make ac susceptibility measurements. The Kappabridge has a coil that produces a magnetic field of 0.0004 T at a frequency of 920 Hz. The sample temperature was scanned at 0.14 K s^{-1} from room temperature to 973 K. With all three magnetometers, measurements were made for bare substrates and the results subtracted from the raw data.

3. Results and discussion

The polarized neutron scans of 10 multilayers are shown in figure 1, in which the normalized intensity of the reflectivity signal is plotted against the momentum transfer normal to the surface defined by $Q = 2k \sin\theta$, where k is the neutron wavenumber and θ is the grazing angle of incidence. The filled and open points correspond to the PNR spin-up and spin-down data respectively, and the lines result from a fitting program that is discussed below. In the figure the scans are presented with the sample showing the smallest interval (ΔQ) between layer peaks plotted top left and successive scans having progressively larger ΔQ intervals. This corresponds to a progressive decrease in (U + Fe) bilayer spacing from top left to bottom right.

The neutron reflectivity scans were analysed with a programme based on the theory of Blundell and Bland [7] and written by Langridge [8]. The input data contains layer thickness, interface thickness, magnetic moment, nuclear scattering length, b, and number density, N. The basic sample structure consists of glass substrate, low density bilayer (U + Fe), stack of (U + Fe) bilayers and two bilayers of low density (U + Fe) oxides.

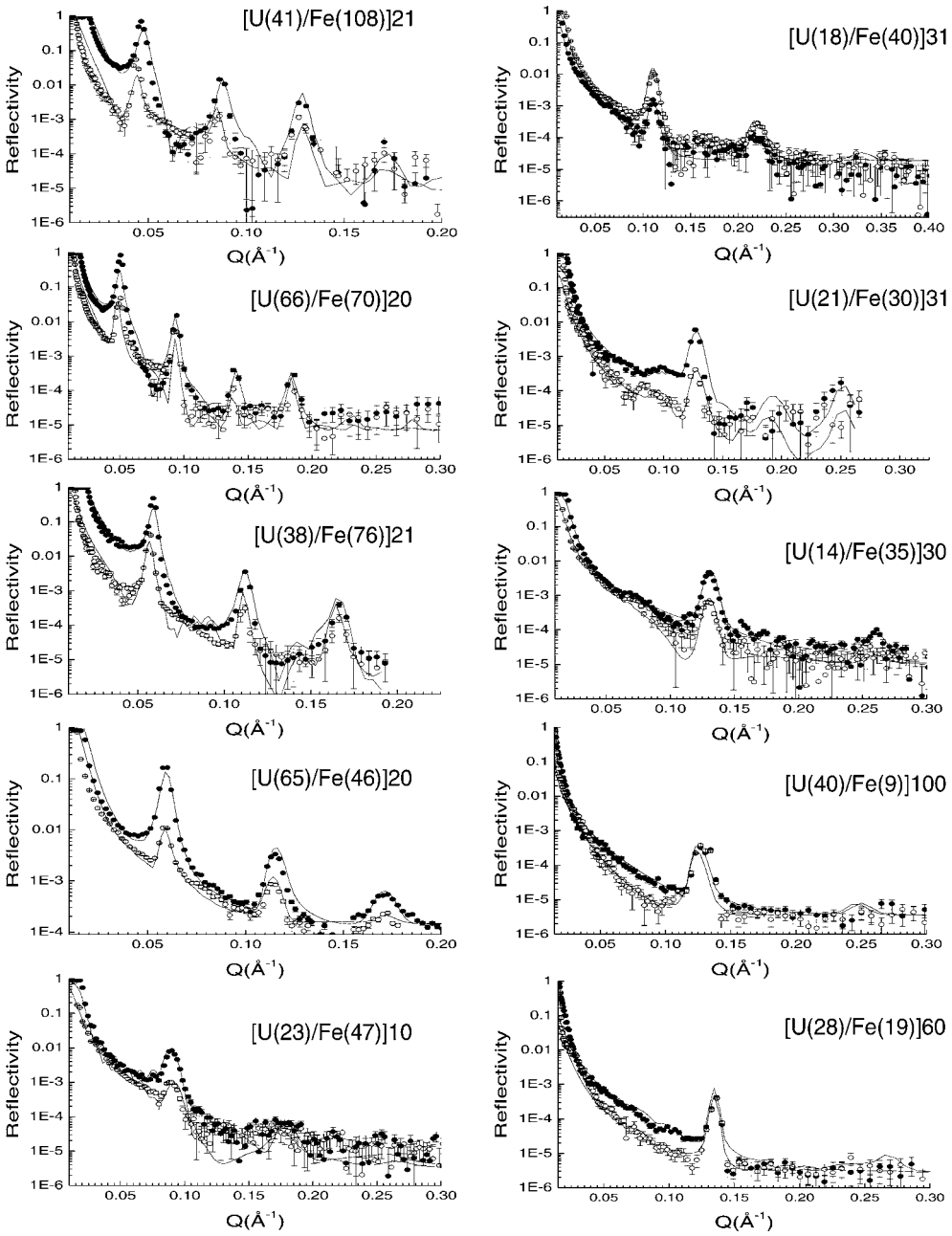

Figure 1. Polarized neutron reflectivity (PNR) scans taken at room temperature. The full points indicate the spin-up and open points the spin-down signal and the lines show the result from the fitting program (three-layer model). These scans are presented in order of decreasing sample bilayer thickness.

The model for the neutron scans was set up to be consistent with the features of the iron layers manifested in the Mössbauer spectra—see paper I [6]. These features are illustrated in the characteristic Mössbauer spectrum of sample 2.11 ([U(14)/Fe(35)]30) shown in figure 2

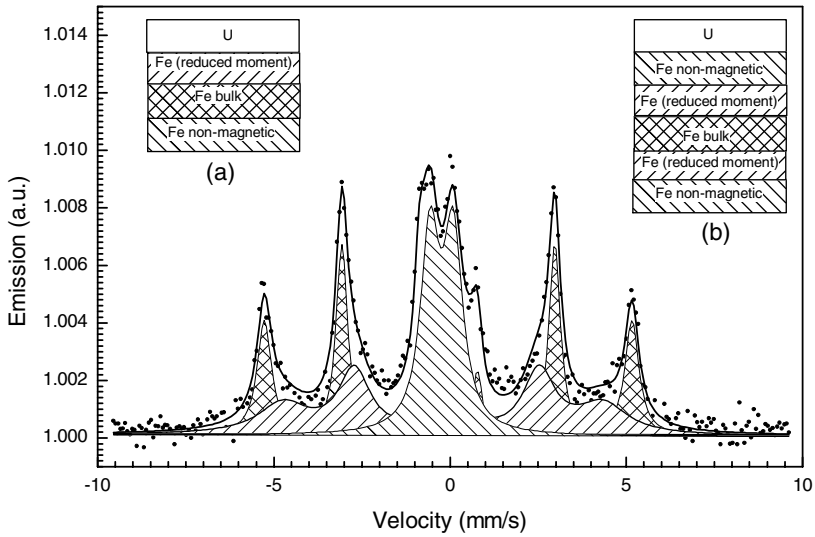

Figure 2. The Mössbauer spectrum of sample 2.11 ([U(14)/Fe(35)]30). There are three components associated with the PNR models with (a) three Fe sublayers and (b) five Fe sublayers. In the figure, correspondence is shown between the layered structures illustrated and the components of the Mössbauer spectrum.

and comprise three components: a component representing well-characterized α-iron with a moment of 2.2 μ_B/atom, a component with a reduced hyperfine field in which the moment per iron atom is reduced and a (probably amorphous) iron component with no moment per iron atom [6]. These features were introduced in the neutron fitting by assigning sublayer components to the iron layers of the stack. As a further refinement, this subdivision of the iron layer into sublayers was made in two alternative ways:

(a) the three-layer model, where the iron layer was split into three sublayers corresponding, in order, to a non-magnetic (zero moment) component, an α-iron component and a reduced moment component; and
(b) the five-layer model, where the iron layer was split symmetrically into five sublayers corresponding to non-magnetic, reduced moment, full α-iron moment, reduced moment and non-magnetic components.

It is seen that in the three-layer model the upper and lower interfaces of the iron layer are different, while in the five-layer model they are the same. In this way, we investigate whether the PNR results are sensitive to possible differences in the interfaces, arising from the fabrication method where, alternately, uranium is deposited on iron and iron is deposited on uranium.

Typical results of fitting with these two models are illustrated in figure 3 for sample 2.4 ([U(41)/Fe(108)]21). It is seen that the fits to the experimental scans using the three-layer model and the five-layer model are equally good: thus PNR does not distinguish between different spatial distributions of the different iron components within the iron layer. This is perhaps not surprising considering the number of parameters already in the fits, and the relatively large error bars in some of the neutron data at large Q. With this established, the fits to the scans in figure 1 were made with the three-layer model. In these fits for the U + Fe stack, the values of b were fixed for the uranium, iron and oxide layers [9]. The number density values, N, were fixed at the U (4.80×10^{28} atoms m^{-3}) and Fe (8.46×10^{28} atoms m^{-3}) bulk

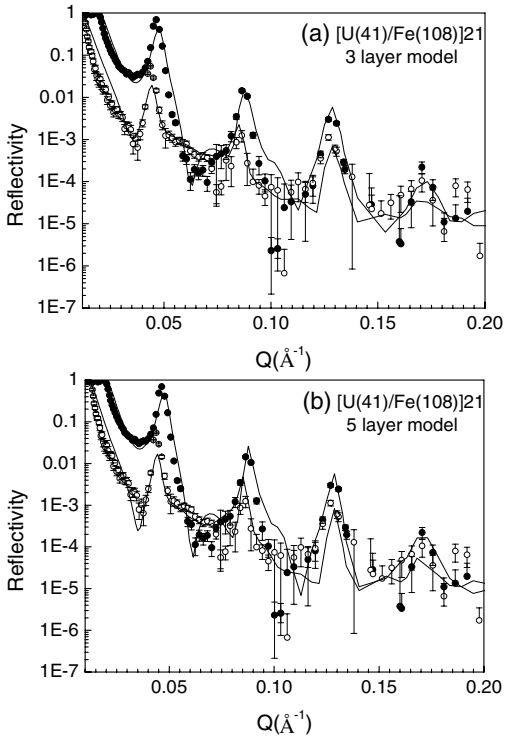

Figure 3. PNR data and fitted curves for sample 2.4 ([U(41)/Fe(108)]21) obtained using the three-layer model (a) and the five-layer model (b).

values for the uranium and bulk α-iron layers in the stack. For the Fe sublayer corresponding to the reduced moment material, N was varied to give the best fit resulting in values around $(7.2 \pm 0.7) \times 10^{28}$ atoms m^{-3}. The number density for the non-magnetic iron atoms at the U/Fe interface was also varied resulting in a value of $(4.5 \pm 1.0) \times 10^{28}$ atoms m^{-3}. Values of thicknesses and optical parameters taken from x-ray reflectivity scans [6] proved good starting points for the neutron fits in all cases.

Values of layer thickness and average magnetic moment are listed in table 1 for a series of multilayers with fitted thicknesses in the range 9 Å $< t_{\mathrm{Fe}} <$ 108 Å and 14 Å $< t_{\mathrm{U}} <$ 66 Å. The consistency of the deduced structural parameters between the two independent measurements with neutrons and x-ray [6] gives confidence in the results at a first level of approximation. More precise characterization tools, RXS for example, may well reveal a more complex layer structure.

Data from the fits to the PNR scans are listed in table 1. The iron and uranium thicknesses t_{Fe} and t_{U}, as well as interface thicknesses $r_{\mathrm{i}}(\langle r_{\mathrm{i}} \rangle \approx 8 \pm 5$ Å), are determined by the fits to the scans. The values of the uranium magnetic moment are not accurately determined from these scans due to the small values and are, in all cases, below the uncertainty of 0.05 μ_{B}. The percentage of magnetic iron atoms in table 1 comes from the relative area of the magnetic components of the Mössbauer spectra. The agreement between the proportion of magnetic iron atoms as assessed by PNR and Mössbauer approaches is demonstrated in figure 4. The mean magnetic moment per iron atom in table 1 is evaluated from an average of the moments of the three components weighted by their respective proportions. In this evaluation the moment per atom of α-iron is taken as 2.2 μ_{B}, that of the non-magnetic iron as zero and that of the

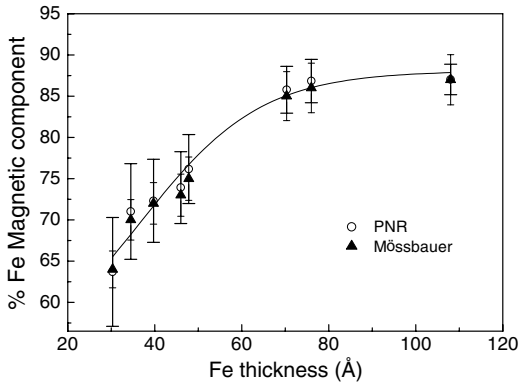

Figure 4. The percentage of the Fe magnetic component (bulk + reduced moment components) as a function of the Fe-layer thickness, obtained from the PNR (circles) and Mössbauer (triangle) measurements. The curve is a guide to the eye.

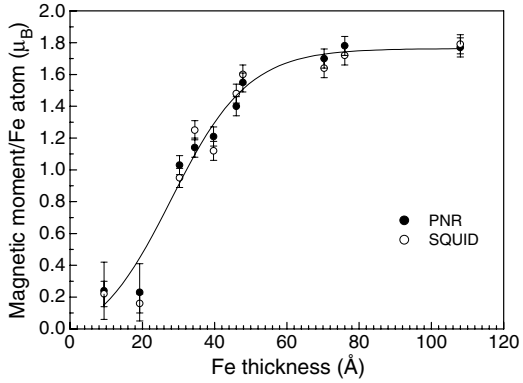

Figure 5. The average magnetic moment per Fe atom obtained from the PNR (open circles) and SQUID (full circles) measurements plotted against the thickness of the iron in the Fe layers. The curve is a guide to the eye.

reduced component as the value arising from the fit to the particular multilayer (in practice, values lie within the range 1.3 ± 0.5 μ_B/Fe atom). The corresponding mean iron atom densities N are listed in table 1. Over the range of multilayers this value of N lies in a range $(6.0–7.9) \times 10^{28}$ atoms m^{-3} compared to the iron bulk value of 8.46×10^{28} atoms m^{-3}. This reduction in mean density of iron atoms in iron multilayer levels has been observed previously, e.g., in Fe/Gd multilayers where a reduction of about 12% is reported [10].

The values of the magnetic moments per Fe atom measured by SQUID magnetometry are listed in table 1. The excellent agreement between the average moments determined by PNR and SQUID measurements is illustrated in figure 5. For Fe-layer thicknesses larger than 60 Å, the observed saturation magnetic moment appears to be constant at about 1.78 μ_B/Fe atom. For decreasing Fe-layer thicknesses below 50 Å, the moment drops rapidly to a near-zero value and, as shown in paper I [6], the Fe for thicknesses less than 18 Å is almost certainly amorphous throughout the layer.

To study the interfacial magnetism in these systems we have employed off-specular neutron diffraction. Briefly, by definition, the true specular reflectivity presented contains

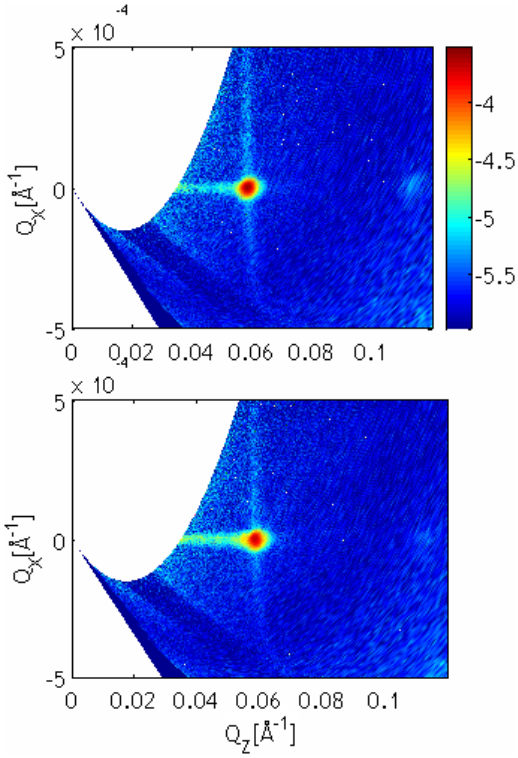

Figure 6. The observed scattering from sample 2.5 ([U(65)/Fe(46)]20) at the coercive field. The top (bottom) panel corresponds to incident neutron spin up (down). The diffuse scattering is clearly visible.

no component of the neutron momentum transfer in the plane of the sample and therefore is not sensitive to the in-plane structure. By transferring momentum into the plane of the sample it is then possible to observe scattering from the in-plane interfacial structure. Figure 6 shows the reciprocal space maps for sample 2.5 ([U(65)/Fe(46)]20). Q_Z is the momentum transfer perpendicular to the surface and Q_X the component in the plane of the sample. $Q_X = 0$ corresponds to the specular reflectivity. For $Q_Z = 0.06$ Å^{-1}, the first-order Bragg reflection is visible. This arises from the structural periodicity of the multilayer and also any magnetization with the same periodicity, e.g., ferromagnetism. (The weaker second-order Bragg peak is also visible.) For figure 6, the sample is at the coercive field and therefore there is no spin dependence to the scattering as demonstrated by the equivalence of the two panels. Strikingly, there is a ridge of scattering running perpendicular to the Bragg peaks arising from a conformal interfacial structure [11]. There is no evidence for uncorrelated interfacial structure. Applying a saturation field (figure 7), the spin asymmetry is clearly visible, at the Bragg peaks, indicating a ferromagnetic ordering of the Fe blocks and also in the diffuse scattering. To quantify this structure [11] we have interpreted this scattering as arising from magnetic roughness in the interfacial region, i.e., the cross-correlation of the structural and magnetic interface. We have assumed a structural correlation length of 200 Å. The results of the calculation are shown in figure 8 for slices taken through the first-order Bragg peak. The in-plane magnetic roughness length scale is 3600 ± 500 Å which is considerably longer than the structural correlation length. The degree of magnetic roughness decreases slightly in going from the coercive to saturation fields.

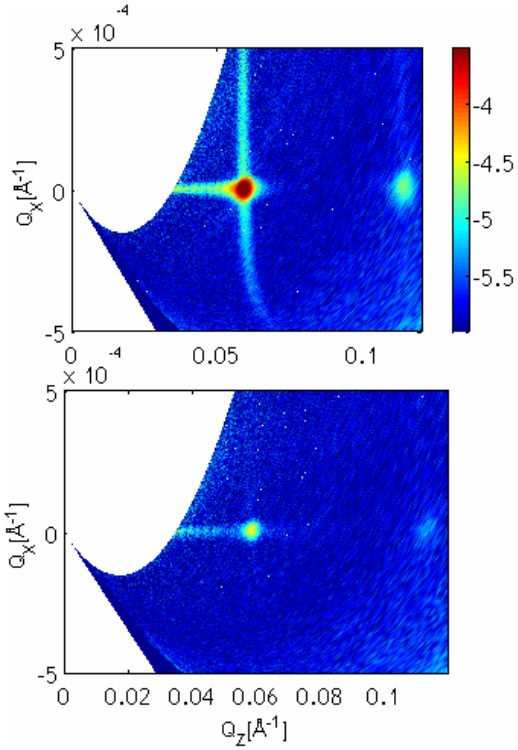

Figure 7. The observed scattering from sample 2.5 ([U(65)/Fe(46)]20) at the saturation field. The top (bottom) panel corresponds to incident neutron spin up (down). The bending of the diffuse ridge is due to refraction of the neutron beam within the sample.

From the preceding analysis, the interfacial chemical structure is vertically correlated throughout the multilayer. At the coercive field, the magnetic interfacial structure effectively smooths out the magnetic interface relative to the structural one, possibly due to the long range nature of the magnetic interaction. There is no evidence for a correlated domain structure (which would suggest magnetic coupling between the Fe layers). As the layer magnetization is saturated, the magnetic roughness is not significantly affected (relative to the specular intensity) suggesting that the interfacial magnetism tracks that of the bulk layers. This also removes the possibility that the observed diffuse scattering is from a domain structure as the sample is now in a single-domain state.

The magnetization versus temperature for the U/Fe multilayers exhibited very little variation, and certainly no magnetic transitions, from 4.2 to 375 K, in applied magnetic fields of 0.005 and 0.1 T. It is observed that the measured signal increases with the thickness of the Fe layer. The magnetization did not show any anomalies when measured from 0 to 7 T at temperatures of 4.2 and 295 K. Representative results of these magnetization measurements are shown in figure 9 for samples 2.4 ([U(41)/Fe(108)]21) and 2.10 ([U(18)/Fe(40)]31). The curves of magnetization are typical of a ferromagnet. In addition, the PNR data show unambiguously that the layers are not antiferromagnetically ordered at room temperature.

Hysteresis loops measured with the applied magnetic field parallel and perpendicular to the surface of the U/Fe multilayers were also taken for the samples listed in table 1. The observed results are very similar for the various multilayers and a typical pair of curves is shown in

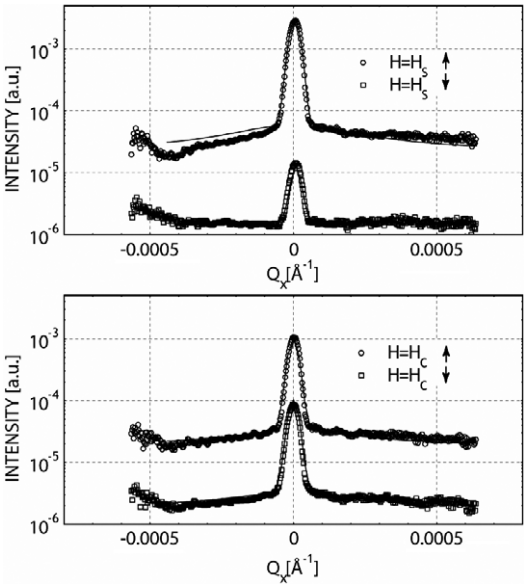

Figure 8. Slices through the first-order Bragg peak for the data presented in figures 6 and 7. The data sets within each panel have been offset by a factor of ten for clarity. The solid curves are fits to the simple model described in the text.

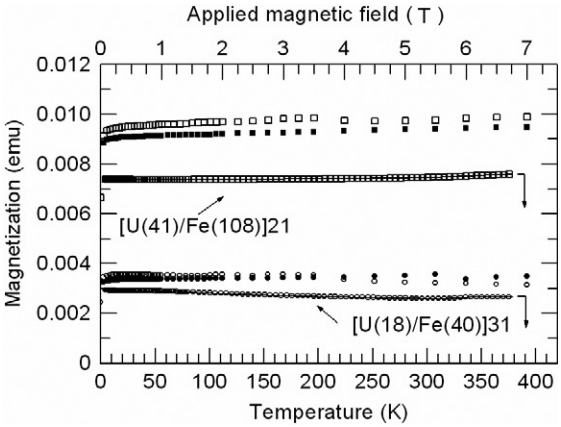

Figure 9. Results of magnetization measurements on sample 2.4 ([U(41)/Fe(108)]21) (squares) and sample 2.10 ([U(18)/Fe(40)]31) (circles) for a temperature scan (strike-through markers, bottom x-axis) with $H = 0.005$ T and an applied field scan (top x-axis) with $T = 4.2$ K (solid points) and 295 K (open points).

figure 10 for multilayer 2.2 ([U(28)/Fe(43)]11). They all exhibited slight magnetic anisotropy between the parallel and perpendicular directions. The results for the example shown indicate a coercivity and saturation moment of 0.004 T and 1.78 μ_B/Fe atom, respectively, in the parallel direction, and 0.054 T and 1.78 μ_B/Fe atom, respectively, in the perpendicular direction. The results of figure 10 are indicative of the easy axis lying in the plane of the multilayer. Other multilayers showed a coercivity of approximately 0.004 T in the parallel direction as well. However, the coercivity in the perpendicular direction increased with increasing Fe-layer thickness, with the result that at a thickness of 100 Å, the coercivity value was 0.070 T.

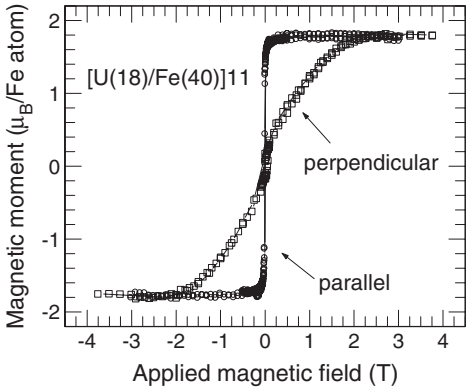

Figure 10. Hysteresis curves for sample 2.2 ([U(18)/Fe(40)]11) for the magnetic field applied perpendicular (open squares) and parallel (open circles) to the plane of the multilayer.

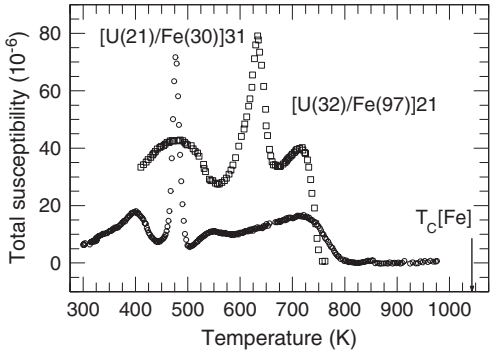

Figure 11. Results of ac susceptibility measurements on multilayers 2.12 ([U(21)/Fe(30)]31) and 2.6 ([U(32)/Fe(97)]21) with T_C of 477 and 634 K, respectively, as compared to the T_C of bulk iron, 1043 K.

The temperature-dependent ac susceptibility χ is also a powerful tool for examining the nature of magnetic phase transitions, such as ferromagnetic transitions. Typically, χ diverges at the critical temperature of a ferromagnetic phase transition. In this study, the total susceptibilities of two multilayers, 2.12 ([U(21)/Fe(30)]31) and 2.6 ([U(31)/Fe(100)]21), were measured from room temperature to 973 K in a 0.4 mT applied magnetic field. The results are shown in figure 11. The Curie temperatures of the multilayers were found to be 477 and 634 K, respectively. These temperatures are significantly reduced from the T_C of bulk iron, 1043 K. This observed reduction in T_C from the bulk value could be partly due to the reduction in Fe moment discussed earlier. Above a temperature of approximately 775 K the susceptibilities were observed to fall towards zero as the samples lost their structure.

4. Conclusions

Well-defined U/Fe multilayers were prepared by dc magnetron sputtering. In the preceding paper (I) we discussed their structural characterization. Their magnetic properties, as studied using polarized neutron reflectometry, off-specular neutron diffraction and SQUID and Mössbauer spectroscopy, have been presented in the present paper. The multilayers exhibit

ferromagnetism with the easy axis in the plane of the multilayer. The magnitude of the Fe moments shows a strong dependence on the thickness of the Fe layers (figure 5). At this stage it is unclear whether this dependence is related to the growth and possible complexity of the Fe layers (see figure 2 and table 1) or to interactions between the Fe and U magnetism across the interlayer interfaces. For example, Mössbauer and transmission electron microscopy on Gd/Fe films [12] have shown that the Fe films are mostly amorphous up to a thickness of about 20 Å. This is because of the interfacial strain across the Gd/Fe interface, rather than arising from interdiffusion. In our case we find a similar value. From this, in analogy with [12], we conclude that in addition to the interdiffusion at the interface, there is probably a small thickness of Fe that is amorphous (and with a reduced density and moment), simply as a result of the strain produced by the growth process.

With the techniques presented so far in papers I and II, we have been unable to observe any magnetism of the U layers. However, an earlier RXS study [5] on one of these samples has already shown that the 5f states are polarized, and so more such studies with RXS, and also with x-ray magnetic dichroism, will be performed. Perhaps not surprisingly, the saturation magnetization was found to increase with increasing Fe-layer thickness and the hysteresis curves exhibited a small degree of perpendicular magnetic anisotropy. For the samples with thinner Fe layers, a considerable reduction in T_C as compared to that for pure Fe was observed; this result is compatible with the reduced Fe moment in such samples.

A future programme will incorporate further studies made on new samples prepared with a four-gun dc magnetic sputtering apparatus. Samples can then be prepared with an inert capping layer, thus avoiding the oxide overlayers that complicate the reflectivity analysis [6]. The system, comprising a two-chamber arrangement evacuated by turbo-molecular pumps, will also provide for rapid substrate loading and this will be coupled with the ability to heat the substrate stage during growth. Magnetotransport measurements are planned, in part to evaluate any possible GMR within these uranium-based multilayers.

Acknowledgments

AMB is grateful for the support of an ORS award. ADFH acknowledges the receipt of an EPSRC research studentship. We would like to thank the local contacts at the ILL (D17) and ISIS (CRISP) facilities for their support during the experiments.

References

[1] Carcia P F, Meinhaldt A D and Suna A 1985 *Appl. Phys. Lett.* **47** 178
[2] Baibich M N, Broto J M, Fert A, Nguyen van Dau F, Petroff F, Eitenne P, Creuzet G, Friederich A and Chazelas J 1988 *Phys. Rev. Lett.* **61** 2472
[3] Jaouen N, Tonnerre J M, Raoux D, Bontempi E, Ortega L, Münzenberg M, Felsch W, Rogalev A, Dürr H A, Dudzik E, van der Laan G, Maruyama H and Suzuki M 2002 *Phys. Rev.* B **66** 134420 and references therein
[4] Fumagalli P, Plaskett T S, Weller D, McGuire T R and Gambino R J 1993 *Phys. Rev. Lett.* **70** 230
[5] Brown S D, Beesley A, Herring A, Mannix D, Thomas M F, Thompson P, Bouchenoire L, Langridge S, Lander G H, Stirling W G, Mirone A, Ward R C C, Wells M R and Zochowski S W 2003 *J. Appl. Phys.* **93** 6519
[6] Beesley A M, Thomas M F, Herring A D F, Ward R C C, Wells M R, Langridge S, Brown S D, Zochowski S W, Bouchenoire L, Stirling W G and Lander G H 2004 *J. Phys.: Condens. Matter* **16** 8491
[7] Blundell S J and Bland J A C 1993 *J. Magn. Magn. Mater.* **121** 185
Felici R, Penfold J, Ward R C and Williams W G 1988 *Appl. Phys.* A **45** 169
[8] Langridge S, Rutherford Appleton Laboratory http://www.rl.ac.uk/largescales/
[9] http://www.ncnr.nist.gov/resources/n-lengths/index.html
[10] Hosoito N, Hashizume H and Ishimatsu N 2002 *J. Phys.: Condens. Matter* **14** 5289
[11] Langridge S, Schmalian J, Marrows C H, Dekadjevi D T and Hickey B J 2000 *Phys. Rev. Lett.* **85** 4964
[12] Landes J, Sauer Ch, Kabius B and Zinn W 1991 *Phys. Rev.* B **44** 8342